Effect of Nanoadditives on the Properties of Partially Stabilized Zirconia

A.G. Mamalis[1], E.S. Hevorkian[2], V.P. Nerubatskyi[3*], M. Rucki[4], Z. Krzysiak[2], O.M. Morozova[3]

[1]Project Center for Nanotechnology and Advanced Engineering, Athens, Greece
[2]University of Life Sciences in Lublin, 13 Akademicka, Lublin 20-950, Poland
[3]Ukrainian State University of Railway Transport, Kharkiv, Ukraine
[4]Kazimierz Pulaski University of Technology and Humanities in Radom, Poland
E-mail: NVP9@i.ua

A comparative analysis of the effect of various nanoadditives on a matrix of zirconium dioxide partially stabilized with Y2O3 during hot pressing by electrosintering is given. The microstructure obtained with different compositions of nanoadditives and sintering modes is investigated. The features of the influence of various nanoadditives from Al2O3, WC and SiC on the microstructure and properties of the obtained materials are revealed. The possibility of using the obtained composite materials, taking into account the peculiarities of mechanical properties, as functionally graded materials is considered.

Keywords: nanopowder, zirconium dioxide, tungsten monocarbide, silicon carbide, electrosintering, microstructure, functionally gradient material.

1. Introduction

The determining factor for the structure of nanocrystalline materials is the extremely small grain size, the resulting large area of the boundaries and, accordingly, the length of their joints per unit volume, the difficulty or suppression of the dislocation mechanisms of plastic deformation at grain sizes below a certain limit value, and the nonequilibrium state of the grain boundaries [1]. The developed surface of isolated nanoparticles initiates size effects of thermodynamic quantities. Due to the existence of a significant number of atoms near the surface of the nanomaterial, as well as the dynamics of the lattice, which undergoes significant changes due to a number of features of the nanostate, such characteristics of the substance as the values of heat capacity [2], thermal conductivity [3, 4], melting temperature, temperature Debye.

Size effects should be understood as a complex of phenomena associated with a change in the properties of a substance due to the actual change in particle size and a simultaneous increase in the share of the surface contribution to the overall properties of the system. Due to the noted structural features, nanocrystalline materials differ significantly in properties from ordinary polycrystals. For this reason, grain size reduction is currently regarded as an effective method for changing the properties of a solid. For example, the combination of high hardness with plasticity in nanocrystalline materials is usually explained by difficulties in activating dislocation sources due to the small size of crystallites, on the one hand, and the presence of grain boundary diffusion creep, on the other hand. Nanomaterials are distinguished by exceptionally high atomic mobility, which is 5…6 orders of magnitude higher than that in ordinary crystals [5], however, the mechanisms of diffusion processes in nanocrystalline substances are far from fully understood, and there are opposite explanations in the literature on this matter. Until now, the issue of the microstructure of nanocrystals, i.e., the structure of interfaces and their atomic density, the effect of nanopores and other free volumes on the properties of nanocrystals, remains debatable. In the technological series "synthesis of nanopowders – molding – sintering", the final product – a consolidated material – is very sensitive to all stages of its prehistory, starting with the quality parameter of nanopowders.

Several parameters of nanopowders are known, which are very important for assessing their quality. The first is the average particle size, the second is the particle size distribution spectrum, which significantly depends on the preparation method. Currently, a lot of research is devoted to zirconium dioxide ZrO2 nanopowders [6, 7]. Traditionally, ZrO2-based ceramics have been used in the metallurgical industry to make crucibles for melting metals. Currently, zirconium ceramics is one of the most promising ceramic materials for structural and tool purposes and is used in the technology of obtaining parts for gas turbine and diesel engines, friction units, pump sealing rings, shutoff valves, and cutting tools. Also, ceramics based on ZrO2 finds application in medicine for the manufacture of implants in bone tissues. It is known that one of the reasons for the high values of mechanical properties is the martensitic phase transformation of the tetragonal phase into a monoclinic phase, initiated by the elastic field of the emerging and propagating crack. Accordingly, part of the elastic energy is spent not on destruction, but on phase transformation. In addition, the tetragonal-monoclinic transformation is accompanied by an increase in volume; the emerging field of compressive stresses also hinders crack propagation. A similar phenomenon of an increase in mechanical properties as a result of a phase transformation is called transformation hardening [8].

The widely used "stabilized" zirconia ceramic (in tetragonal or cubic form) is a solid solution of the stabilizer oxide in ZrO2 in varying concentrations. Y2O3, MgO, CaO, CeO2 should be noted among the most effective additives [9–11]. Thus, for example, experimental results make it possible to recommend ceramics based on the ZrO2–CeO2 system for creating solid electrolytes [12].

One of the promising materials for the manufacture of multifunctional ceramics is zirconium dioxide partially stabilized with yttrium oxide – ZrO2–Y2O3. Technical ceramics made from

powders based on zirconium dioxide partially stabilized with yttria has a unique set of physical and mechanical properties: high strength, hardness and fracture toughness, resistance to corrosion and wear. Partially stabilized zirconia has a high thermal stability, and thus is also suitable for use at high temperatures in mechanical engineering (including as thermal coatings) [13].

Along with traditionally used stabilizers, aluminum oxide and refractory metal carbides are used to improve some properties, in particular mechanical ones [14, 15]. From numerous publications on this topic, the question arises which of these additives is the most effective in terms of improving mechanical properties. For some reason, less attention is paid to issues of thermophysical characteristics, although recently zirconium dioxide has also found other applications, in particular, in medicine and solid electrolytes.

There is a large amount of experimental data showing the positive effect of small additions of Al2O3 on the mechanical strength of zirconia ceramics [16].

In Table 1 presents some of the physical and mechanical properties of some materials.

Table 1. Physical and mechanical properties of some materials [17]

Material	Density γ, g/cm^3	Young's modulus E, GPa	Thermal expansion coefficient α, $10^{-6}\cdot K^{-1}$	Specific heat C, J/kg·°K	Thermal conductivity λ, W/m·K
ZrO_2	5.6	6.0	10	400	2.5
Al_2O_3	3.8	1.8	8	780	28
WC	15.6	4.7	3.9	184	29.3
SiC	3.05	0.2	4	695	80

The main materials that are widely studied are aluminum oxide (Al2O3), tungsten carbide (WC), silicon carbide (SiC) [18, 19]. This is explained by the fact that systems of two non-interacting solid phases uniformly distributed in the volume are characterized by increased plasticity and impact strength.

Obviously, since sintering is carried out at high temperatures of 1400…1700 °C, the thermophysical properties of the initial powders play a significant role in the obtained composite materials [20].

For example, the smaller the difference in the coefficients of thermal expansion, heat capacity and thermal conductivity, the more compatible the components of this composite. In the formation of mechanical properties, respectively, an important role is played by the elastic moduli of the initial components. And in this case, it is necessary to be able to theoretically calculate the estimated Young's modulus of the resulting composite material. This fact refers primarily to the ZrO2–Al2O3 system, in which the degree of interaction between the components is low, which, accordingly, provides an increased stability of the grain boundary structure [21]. As a result, the ZrO2–Al2O3 binary system is one of the promising composite ceramics with high mechanical properties.

There are works in which the possibility of obtaining ceramics based on systems of the type "ZrO2 – stabilizing oxide – Al2O3" is studied, which corresponds in terms of density, strength and heat resistance to the requirements necessary for ceramics in mechanical

engineering [22]. In addition, aluminum oxide has a stabilizing effect on the tetragonal and cubic modifications of ZrO2 [23].

It is known that refractory transition metal carbides with a significant proportion of the ionic component of the chemical bond have low adhesion to metals and compatibility with oxides, they conduct electric current and are promising as additives to ceramics based on ZrO2 [24, 25]. Additives of carbides, especially in the ultrafine state, can modify the structure and improve the mechanical and tribological characteristics, and also make it possible to obtain materials with an increased level of thermal and electrical conductivity [26, 27].

Therefore, it is completely objective to assume high mechanical properties when ZrO2 is strengthened by nanoparticles of another carbide, WC, and the subsequent prospects for the use of the obtained ceramics. It is known that tungsten carbide is widely used in the manufacture of hard alloys based on WC–Co due to their high wear resistance and low temperatures during application. However, the poor thermal stability of the cobalt binder largely limits its use as a structural component, where high heat resistance, oxidation and corrosion resistance are required. Previously, attention was focused on establishing the optimal amount of ZrO2 in WC-based composite materials obtained by electrosintering [28, 29]. It was also reported in [30] that a 30 % addition of micron-sized WC to the ZrO2 matrix significantly increases the hardness.

It is known that grain boundary diffusion, to a greater extent than diffusion over the volume of grains, is the determining factor affecting the compaction and growth of ceramic grains. Controlling the coefficient of grain boundary diffusion is possible by influencing the free volume of grain boundaries. The main methods for changing the free volume of grain boundaries are associated with microalloying the boundaries with impurity atoms and organizing dislocation flows to the boundaries [31]. The latter mechanism is activated in two ways: providing plastic deformation by applying an external load and using the anisotropy of thermal expansion of ceramic materials (high temperature gradients inside the powder). That is, as previously established in [32], the method of hot pressing with direct current transmission makes it possible to organize the consolidation process in such a way as to avoid problems associated with excessive intensity of grain boundary diffusion: grain growth, leading to an increase in the diffusion path along the boundary, which slows down the sintering process. And the possibility of avoiding abnormal growth (exceeding the average size by some grains) makes it possible to obtain materials with high mechanical properties. Each of the additives to zirconium dioxide separately significantly affects the physical and mechanical properties.

2. Materials and methods

The study used ZrO2 nanopowders partially stabilized with 3 wt.% Y2O3 produced by the Donetsk Institute of Physics and Technology (Ukraine) (Fig. 1).

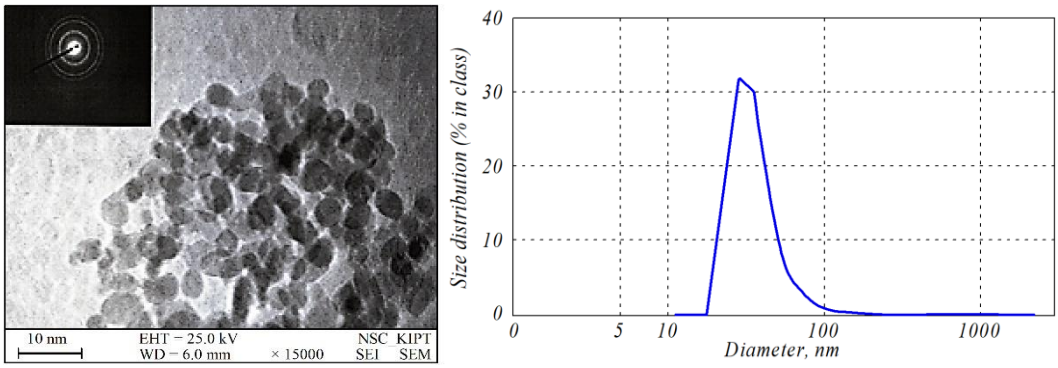

A B

Figure 1. Appearance of ZrO2 nanoparticles (A) and their size distribution (B)

Also used SiC nanopowders manufactured by NANOE (France) (Fig. 2, Table 2), tungsten monocarbide nanopowder manufactured by Wolfram (Austria) (Fig. 3) and SiC powder of the brand NANO SiC CAS # 409-21-2 Saint Gobain (France) (Fig. 4).

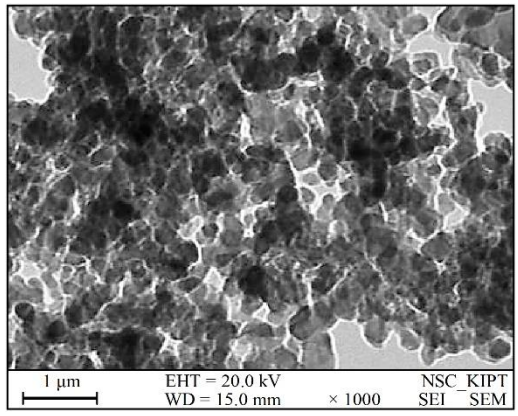

Figure 2. Appearance and characteristics of α–Al2O3 nanoparticles produced by NANOE

Table 2. Chemical composition of α–Al2O3 nanoparticles

Purity	Unit	Al100-BA, Al100
Al_2O_3	wt.%	99.9
MgO	ppm	1000
CaO	ppm	< 200
K_2O	ppm	< 200
Fe_2O_3	ppm	< 50
Na_2O, SiO_2	ppm	< 40

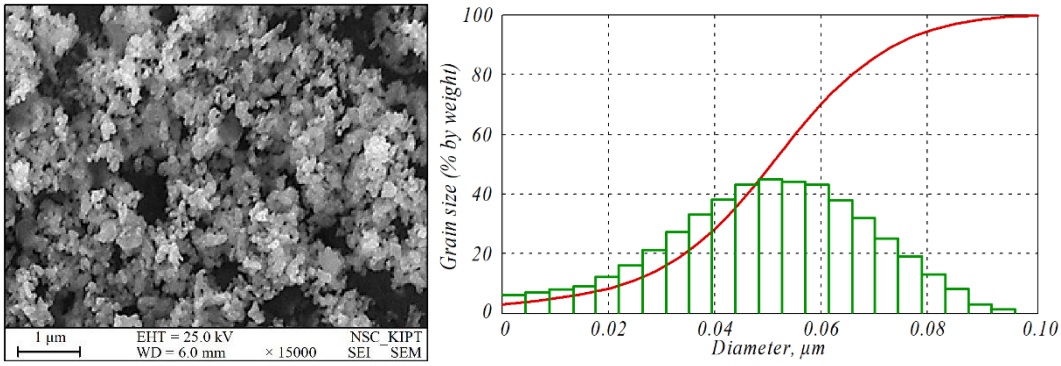

A B

Figure 3. Tungsten monocarbide nanopowder (A), produced by Wolfram (Austria) and histogram of distribution of its fractions (B)

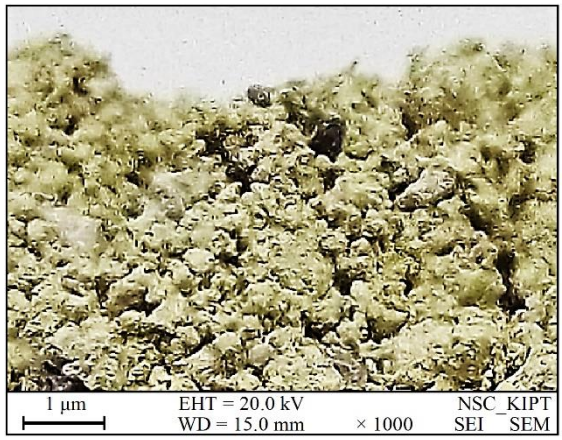

Figure 4. SiC powder brand NANO SiC CAS # 409-21-2

In study, for the molding of ceramic products, a device for hot vacuum pressing with direct current transmission was used, developed and manufactured at the enterprise NPO Kermet-U (Ukraine) [33].

The polishing of the samples was carried out on a Struers grinding and polishing complex (Denmark) using diamond pastes successively up to 1 μm. The structure of electroconsolidated zirconium ceramic samples was studied using force probe (atomic force microscope Ntegra Aura) and scanning (scanning ion-electron microscope Nova NanoSEM, scanning electron microscope Quanta 200 3D) microscopy.

X-ray phase analysis was carried out on a Shimadzu XRD-6000 diffractometer with the following modes: CuKα radiation with $\lambda = 1.54187$ Å; curved graphite monochromator in front of the counter; method $\theta - 2\theta$ of continuous scanning; scanning speed 1.2°/min angular range $2\theta = 5\ldots100°$ with a step of 0.02°; X-ray tube voltage 40 kV, current 30 mA; without sample rotation. Phase analysis of the samples was performed using the ASTM (American Society for Testing Materials) database.

The values of microhardness and crack resistance were determined by measuring the diagonal of the imprint and the length of radial cracks obtained by indentation with a diamond indenter in the form of a tetrahedral pyramid with an apex angle α = 136° (Vickers pyramid) using an AFFRI DM8 automatic microhardness tester. The microhardness value was calculated according to the formula [34, 35]:

$$H_V = \frac{k \cdot P}{(2 \cdot a)^2}, \tag{1}$$

where P is the load on the indenter, kg; 2·a is the average value of the lengths of both diagonals of the imprint, μm; k is the coefficient depending on the shape of the indenter, for the Vickers pyramid k = 1.854.

The fracture toughness coefficient K1C, which characterizes the fracture toughness of the sample, was determined by the formula [36, 37]:

$$K_{1C} = 0.016 \cdot \left(\frac{l}{a}\right)^{-0.5} \cdot \left(\frac{H_v}{E \cdot F}\right)^{-0.4} \cdot \frac{H_v \cdot a^{0.5}}{F}, \tag{2}$$

given that

$$0.25 \le \frac{l}{a} \le 2.5, \tag{3}$$

where E is the Young's modulus, GPa; HV is the microhardness, GPa; F is a constant, F ≈ 3; l is the crack length from the corner of the Vickers pyramid imprint, m; a is the half-diagonal of the Vickers pyramid imprint, the average distance from the imprint center to the end of the crack, m.

Porosity was determined by the formula [38]:

$$P = \left(1 - \frac{\rho}{\rho_n}\right) \cdot 100\ \%, \tag{4}$$

where ρn is the theoretical (X-ray) density of the non-porous material; ρ is the density of the powder compact.

3. Theoretical background

An analysis of the structure of ZrO2 (3 wt.% Y2O3) – Al2O3 nanocomposites shows that the grain size in the samples obtained at temperatures above 1200 °C increased significantly. It is known that the coarsening of powder particles is superimposed on the process of growth of interparticle contacts due to other processes, namely, coalescence and coagulation, each of which can prevail over the other during sintering [39]. Apparently, it was the coagulation process that had a greater effect on the compaction of the system, which is confirmed by our studies during the sintering of ZrO2–Al2O3, the microstructures of the samples of which are shown (Fig. 5), which show that particles stick together with the formation of primary (and in some cases and secondary) aggregates in which the particles have not lost their individuality. In some places, pores are observed between the particles, which is due to

insufficient pressing pressure (35 MPa) and temperature.

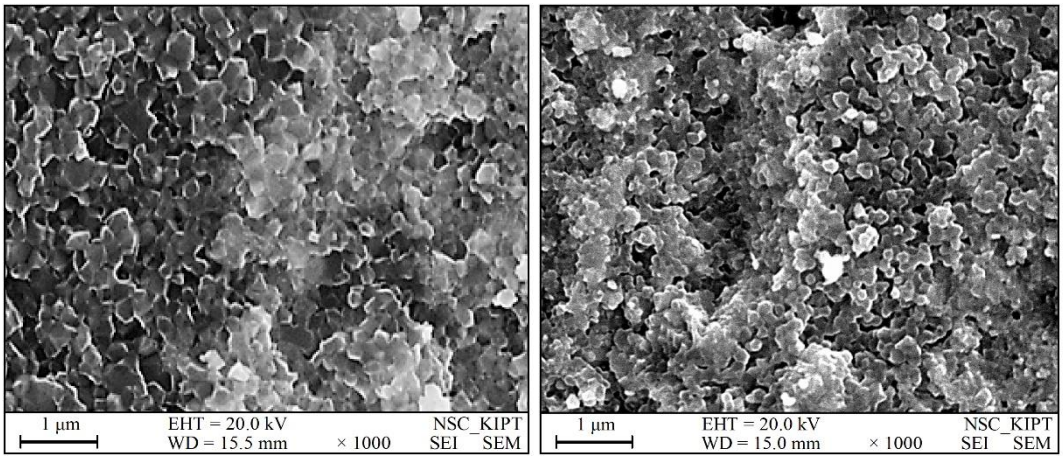

A B

Figure 5. Microstructure of samples from the compositions ZrO2 (A) and ZrO2–10 wt.% Al2O3 (B)

The coalescence process is typical for samples, and at the initial stage of consolidation it competes with the shrinkage process. In electrosintering, shrinkage is activated by heating the workpiece with an industrial frequency current of 50 Hz. This leads to a significant decrease in the yield strength, and hence the production of a denser material at the same pressure. This feature is associated with the intensification of grain boundary diffusion, which leads to the prevalence of compaction processes due to the removal of open porosity over the ceramic grain growth processes [40]. Also, it can be assumed that, just as a change in the heating rate leads to an increase in the temperature gradient inside the sintered powder, creating a local mismatch in the thermal expansion coefficients, so a significant mismatch in the thermal expansion coefficients of the zirconium oxide and aluminum oxide powder particles leads to the movement of dislocations to the emerging boundaries, increasing their free volume and the coefficient of grain boundary diffusion.

An analysis of the phase composition, along with the morphology and dispersion of powders, makes it possible to predict the performance properties of products already at the initial stage of obtaining materials [41, 42].

Investigating the X-ray patterns of the polished surface of the consolidated samples of ZrO2–Al2O3 ceramics (Fig. 6), it was found that the phase composition is characterized by the presence of peaks of monoclinic, tetragonal zirconium dioxide and aluminum oxide in various ratios depending on the temperature of electrosintering (electroconsolidation) and the amount of aluminum oxide in the initial powder mixtures.

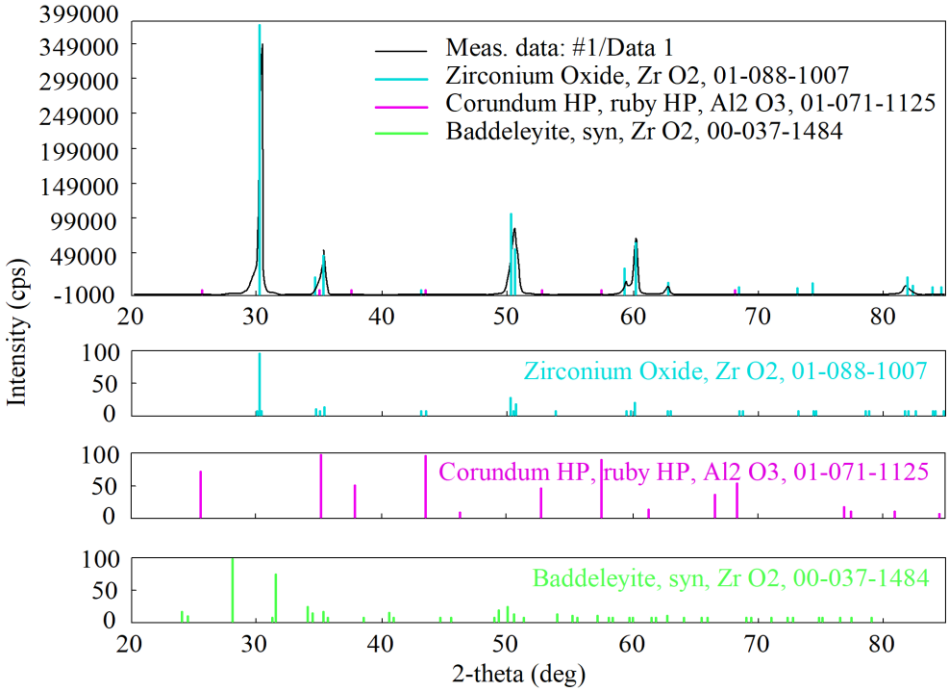
Meas. data: #1/Data 1
Zirconium Oxide, Zr O2, 01-088-1007
Corundum HP, ruby HP, Al2 O3, 01-071-1125
Baddeleyite, syn, Zr O2, 00-037-1484
Intensity (cps)
2-theta (deg)

A

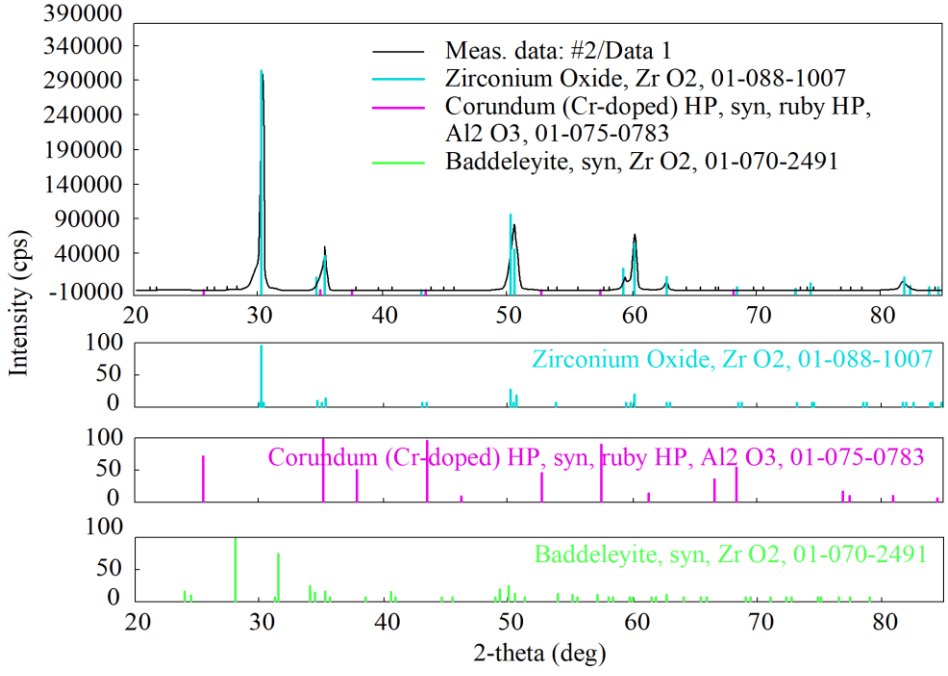
Meas. data: #2/Data 1
Zirconium Oxide, Zr O2, 01-088-1007
Corundum (Cr-doped) HP, syn, ruby HP, Al2 O3, 01-075-0783
Baddeleyite, syn, Zr O2, 01-070-2491
Intensity (cps)
2-theta (deg)

B

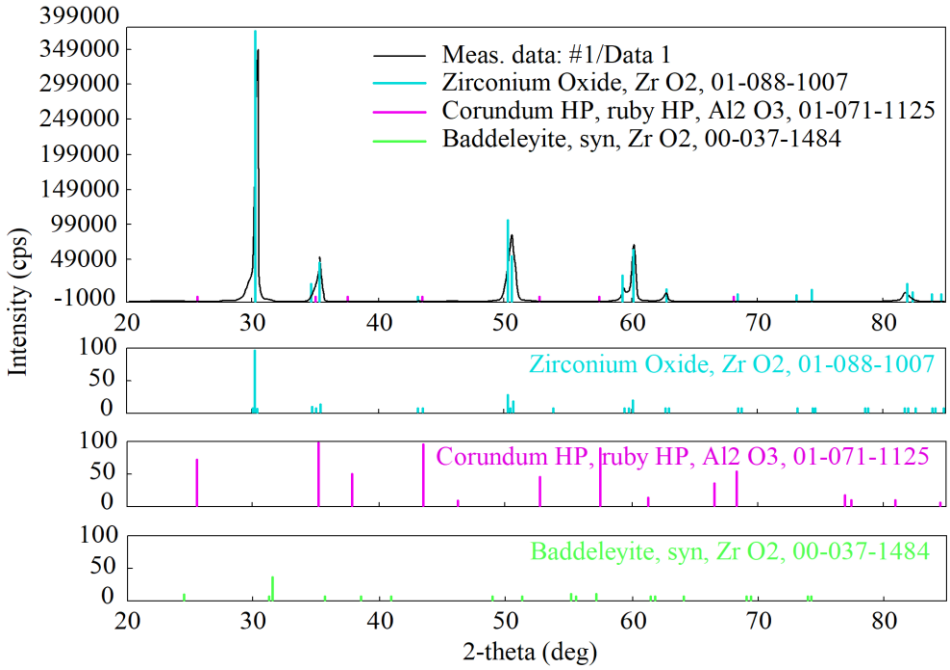

C

Figure 6. X-ray pattern of the polished surface of a sample obtained at a temperature of 1250 °C and containing 10 wt.% Al2O3 (A), 20 wt.% Al2O3 (B) and 30 wt.% Al2O3 (C)

Considering the X-ray diffraction patterns of the samples obtained at a temperature of 1200 °C by hot pressing with the passage of a high-ampere current with a different content of aluminum oxide (Fig. 6), it can be seen that with an increase in the content of Al2O3 from 10 wt.% to 20 wt.%, the content of the monoclinic phase increases , and at a content of 30 wt.% in the sample obtained at a temperature of 1250 °C, it decreases almost to zero.

4. Results and discussion

Some researchers believe that with an increase in the content of the monoclinic phase of zirconium dioxide, the strength of the composite should decrease due to the fact that the volume of the monoclinic phase is greater than the volume of the tetragonal phase, and, obviously, by creating compressive forces in the volume of the composite, the internal stresses of the system increase, and this is in ultimately contributes to a decrease in the strength of the material [9, 43].

In the case under study, this does not occur due to the influence of the addition of aluminum oxide nanopowders, which, apparently, somewhat distorts the crystal structure of tetragonal zirconium oxide, thereby increasing it and thereby compensating for the pressure of the monoclinic phase.

The presence of a certain amount of the monoclinic phase indicates a polymorphic

transformation of tetragonal zirconium dioxide into a low-temperature modification during cooling. The partial transformation could also be facilitated by the low cooling rate of the samples, which, according to [44], does not favor the fixation of high-temperature phases. It is known that in addition to external energy sources (electric current), the appearance of additional internal heat sources (polymorphic transformation occurs with heat release) helps to reduce the temperature and accelerates the sintering process.

The influence of aluminum oxide at a content of up to 30 wt.% also affects the fact that the monoclinic phase is completely transformed into a tetragonal one. This can be explained by the fact that under the influence of a high-ampere electric current during hot pressing, the temperature rapidly rises, and already at 800 °C, partially stabilized zirconia begins to conduct current due to the mobility of ions [45]. The passage of an electric high-ampere current significantly activates the sintering process, contributing to the grain-boundary sliding of aluminum oxide nanopowders and the complete transformation of the monoclinic phase of zirconium dioxide into a tetragonal one. In fact, zirconium oxide, becoming conductive with increasing temperature, contributes to percolation effects when an electric current is passed. The electric current promotes the surface activity of nanopowders, and its variable value contributes to the partial crushing of agglomerated grains, thus affecting the structure formation of composites. Naturally, the structure is affected by the final sintering temperature. It should be noted that with an increase in the sintering temperature, the content of the monoclinic phase also decreases, which passes into the tetragonal one.

On the X-ray diffraction pattern of the test sample, obtained at a temperature of 1250 °C and containing 30 wt.% Al2O3, there were reflections belonging only to tetragonal zirconium oxide (Fig. 7). Since the cooling time did not depend on the concentration of aluminum oxide in the initial powder, then, consequently, the amount of tetragonal ZrO2 in the test sample increased with an increase in the concentration of Al2O3 in the initial powders.

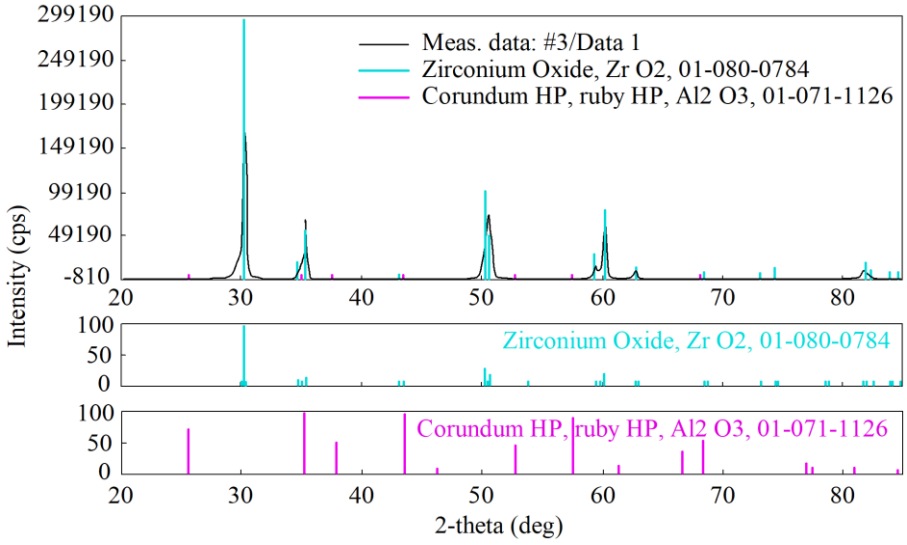

Figure 7. X-ray pattern of the polished surface of the sample obtained at a temperature of 1200 °C and containing 30 wt.% Al2O3

Interestingly, the fracture phase composition of this sample is characterized by the presence of low-intensity peaks of monoclinic zirconium oxide (Fig. 8), and the fracture surface has intergranular fracture regions inherent in the presence of a low-temperature phase.

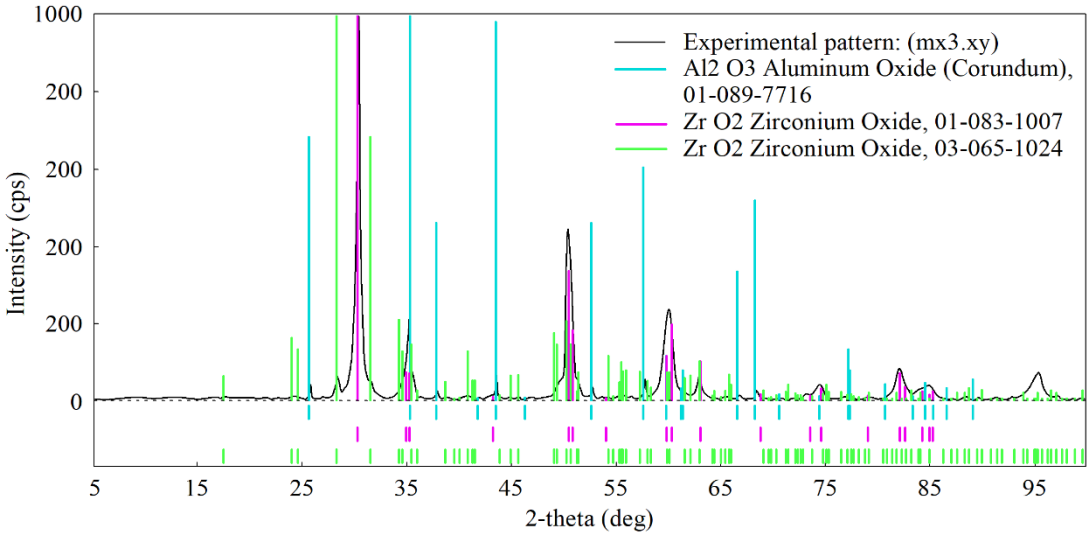

Figure 8. X-ray pattern of the destruction surface of a sample obtained at a temperature of 1300 °C and containing 30 wt.% Al2O3

These facts indicate that a tetragonal-monoclinic transformation takes place during loading. That is, the addition of 30 wt.% alumina contributes to the strengthening of the material based on zirconium oxide while restraining abnormal grain growth and forming a finer structure with a high content of the tetragonal phase, capable of transformation into a monoclinic phase (under the action of stresses) near the crack tip. Additives of 30 wt.% alumina contribute to the strengthening of the material based on zirconium oxide while restraining abnormal grain growth and the formation of a finer structure with a high content of the tetragonal phase, capable of transformation into a monoclinic phase (under the action of stresses) near the crack tip. The results of measuring the mechanical properties of some composites are shown in the table, which presents the results for hot pressing by electrosintering, when the maximum pressure on the graphite mold is 40 MPa, and the sintering time at the maximum temperature is 2 minutes.

In Table 3 presents of the mechanical properties of the sintered composites with Al2O3.

Table 3. Mechanical properties of the sintered composites with Al2O3

Composite composition	Sintering temperature, °C	Relative density	Hardness HV_{10}, GPa	Fracture toughness K_{IC}, MPa·m$^{1/2}$
ZrO_2 – 10 wt.% Al_2O_3	1200	0.85	8.2±0.03	4.5±0.1
ZrO_2 – 20 wt.% Al_2O_3	1200	0.86	8.5±0.03	4.8±0.1
ZrO_2 – 30 wt.% Al_2O_3	1200	0.88	8.5±0.03	5.5±0.1
ZrO_2 – 10 wt.% Al_2O_3	1400	0.91	10.5±0.03	9.5±0.1
ZrO_2 – 20 wt.% Al_2O_3	1400	0.95	12.5±0.03	10.2±0.1

ZrO_2 – 30 wt.% Al_2O_3	1400	0.96	12.8±0.03	11±0.1
ZrO_2 – 10 wt.% Al_2O_3	1500	0.95	12.9±0.03	12±0.1
ZrO_2 – 20 wt.% Al_2O_3	1500	0.96	13.1±0.03	12.5±0.1
ZrO_2 – 30 wt.% Al_2O_3	1500	0.98	13.3±0.03	13±0.1
ZrO_2 – 10 wt.% Al_2O_3	1600	0.98	13.5±0.03	13.5±0.1
ZrO_2 – 20 wt.% Al_2O_3	1600	0.99	13.5±0.03	13.8±0.1
ZrO_2 – 30 wt.% Al_2O_3	1600	0.99	13.6±0.03	14.6±0.1

The study of the effect of tungsten monocarbide nanopowders on the properties of zirconium dioxide partially stabilized with yttria is topical due to the fact that tungsten monocarbide has high hardness and abrasive resistance; therefore, it is expected that the introduction of this additive will increase the wear resistance and fracture toughness of the composite as a whole [46].

It should be noted that tungsten monocarbide conducts electric current, and, therefore, can introduce positive dynamics into the mechanisms of sintering of nanopowder mixtures during hot pressing with direct transmission of high current. Hot pressing processes with mixtures with different contents of tungsten monocarbide at different temperatures and holding times were investigated. The pressure in this case was the maximum that this graphite mold can withstand. In all samples, the pore structure is represented by closed spherical (or close to spherical) pores and pore clusters (a set of communicating pores). Pore clusters are formed mainly around spherical grains and only for samples containing 20 wt.% WC and 30 wt.% WC, consolidated at a temperature of 1400 °C and 1500 °C, respectively. These grains have a size from 250 nm to 370 nm, which is 10 times larger than the size of spherical particles in the original powder, and they, as a rule, do not have pores inside them. Samples consolidated at a temperature of 1600 °C had the minimum porosity. The nature of compaction of composites with different contents of tungsten carbide, in comparison with samples of partially stabilized zirconium oxide without additives, was presented in [47].

All composites are characterized by full compaction after a holding time of 2 min. Pure ZrO2 reaches its full density even before the sintering temperature at a maximum pressure of 40 MPa.

It is known that the thermal conductivity of pure tungsten carbide increases with increasing temperature from 20 to 40 W/m·K–1, while the thermal conductivity of zirconium oxide is very low (2 W/m·K–1) and does not change with increasing temperature. In this regard, the thermal conductivity of dense composites also increases depending on temperature. The electrical conductivity of tungsten carbide also increases with temperature and is always several times (2…3 times) higher than pure zirconium oxide, that is, the effect of the content of tungsten carbide in composites based on zirconium oxide is also significant.

The volume content in all samples was 0.6; 0.69; 0.76 for compositions with 10, 20 and 30 wt.% WC, respectively, which significantly exceeded the percolation threshold (≈ 0.33). Thus, there is a noticeable difference in current distribution between pure zirconia and tungsten carbide samples. The different current path during electroconsolidation greatly affects the processes of heat generation and the internal effects of mass transfer in the material.

In the case of a non-conductive pure zirconia sample, Joule heating does not occur; the initial

heating of the sample is not performed by current, in contrast to the case with samples with tungsten carbide, where Joule heating begins immediately, i.e., the formation of the structure occurs mainly already in the process of heating to the holding temperature. The high heating rate minimizes the effect of diffusion processes on the surface of the particles, which do not contribute to compaction, and the samples reach high temperatures faster, while maintaining the ability to sinter. That is, rapid heating accelerates densification due to earlier activation of dislocation creep mechanisms and due to shortening of the low temperature sintering stage when surface diffusion dominates.

From Table 4 it can be seen that the maximum density, close to theoretical, of the ZrO2–10 wt.% WC and ZrO2–20 wt.% WC samples is achieved at a sintering temperature of 1500 °C and 1600 °C, respectively, while the effect of holding time at these temperatures density is less significant.

Table 4. Mechanical properties of sintered composites with WC

Composite composition	Sintering temperature, °C	Relative density	Hardness HV_{10}, GPa	Fracture toughness K_{1C}, MPa·m$^{1/2}$
ZrO_2 – 10 wt.% WC	1400	0.81	9.2±0.03	6.3±0.1
ZrO_2 – 20 wt.% WC	1400	0.79	9.6±0.03	7.5±0.1
ZrO_2 – 30 wt.% WC	1400	0.76	10.8±0.03	7.1±0.1
ZrO_2 – 10 wt.% WC	1500	0.95	11.2±0.03	8.5±0.1
ZrO_2 – 20 wt.% WC	1500	0.95	12.5±0.03	9.3±0.1
ZrO_2 – 30 wt.% WC	1500	0.94	13.2±0.03	9.1±0.1
ZrO_2 – 10 wt.% WC	1600	0.98	13.5±0.03	9.2±0.1
ZrO_2 – 20 wt.% WC	1600	0.98	14.2±0.03	9.1±0.1
ZrO_2 – 30 wt.% WC	1600	0.99	14.5±0.03	8.6±0.1

The decrease in fracture toughness with increasing tungsten monocarbide content (Fig. 9) can be explained by an increase in W2C content. Some mechanical properties of composites of different compositions are given in the table, where the samples were obtained at a maximum pressure of 40 MPa and a holding time of 2 min.

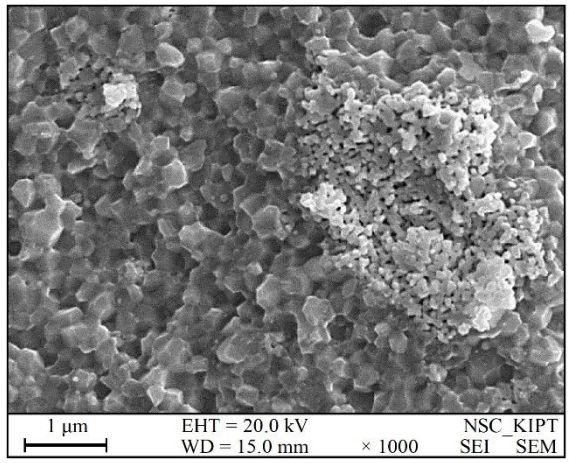

Figure 9. Fracture of a ZrO2 sample – 30 wt.% WC, sintered at T = 1500 °C, P = 30 MPa, sintering time 2 min

An interesting additive in the sintering of zirconium dioxide is silicon carbide [48–50]. The effect of silicon carbide nanopowders on the properties of zirconium dioxide differs significantly from the effect of tungsten nanocarbide additives. On Fig. 10 shows the fracture structure of a specimen sintered at T = 1500 °C. Some elongated grains of silicon carbide, resembling fibers, are noticeable in the structure. Perhaps, during sintering, anomalous growth occurs in one of the crystallographic directions; further studies are required to clarify this phenomenon, primarily the morphology of the initial silicon carbide nanograins.

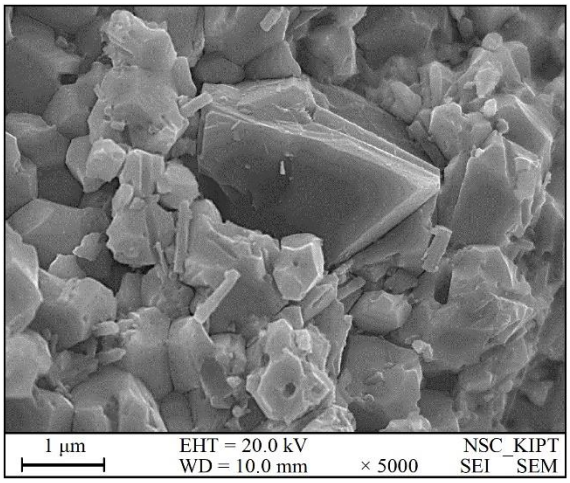

Figure 10. Fracture pattern of ZrO2–20 wt.% SiC composite sintered at T = 1500 °C, P = 35 MPa, holding time 3 min

From Fig. 11, Fig. 12, Fig. 13 clearly shows how the chemical elements are distributed, as well as the chemical composition in different parts of the sample. This distribution practically remained the same at a higher sintering temperature of 1600 °C.

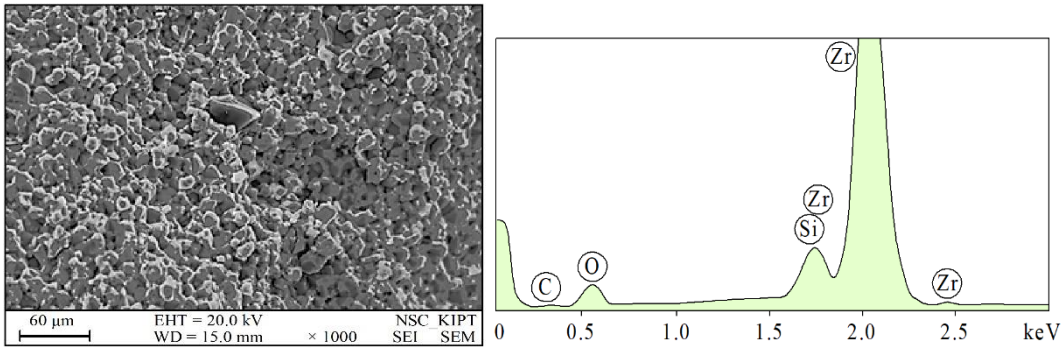

A B

Figure 11. Microstructure of (A) ZrO2–20 wt.% SiC sample sintered at T = 1500 °C, pressure P = 35 MPa, holding time 3 min, (B) intensity of distribution of elements at point 1

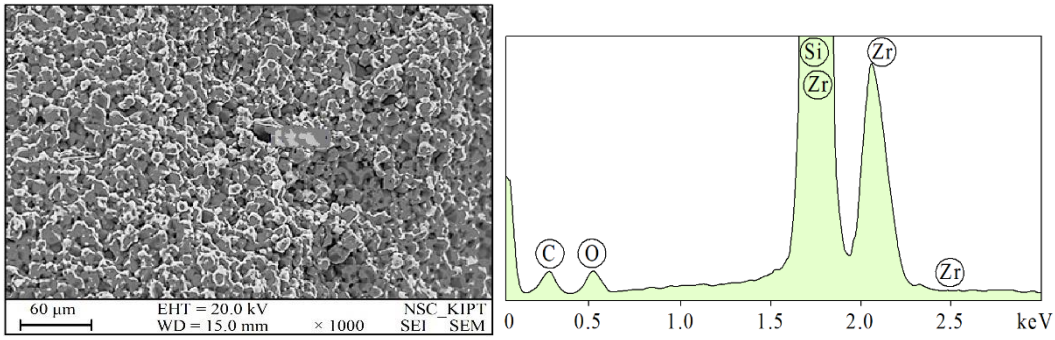

Figure 12. Microstructure of (A) ZrO2–20 wt.% SiC sample sintered at T = 1500 °C, pressure P = 35 MPa, holding time 3 min, (B) intensity of distribution of elements at point 2

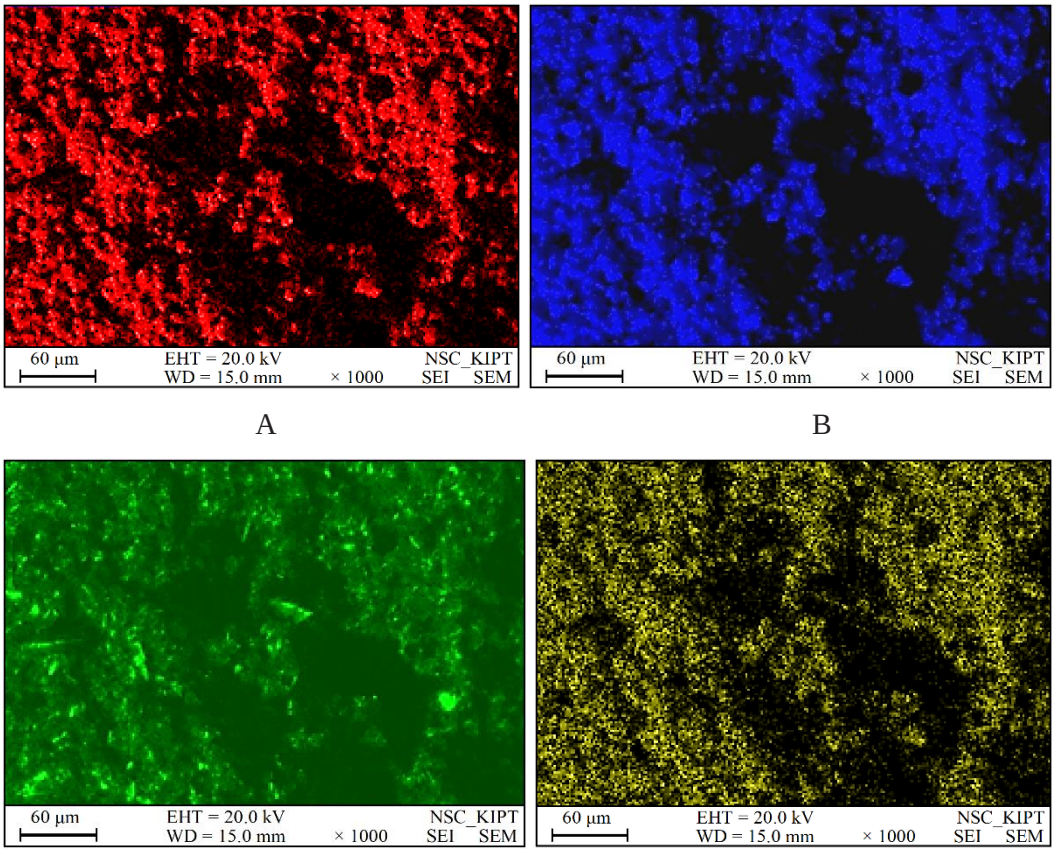

Figure 13. Spectral analysis of the distribution of elements in a ZrO2–20 wt.% SiC sample sintered at T = 1500 °C, pressure P = 35 MPa, holding time 3 min: (A) element O K; (B) Zr L element; (C) element Si K; (D) element C K

The distribution of chemical elements in the ZrO2–20 wt.% SiC composite sintered at T = 1500 °C, P = 35 MPa, holding time 3 min for point 1 is presented in Table 5, for point 2 – in Table 6.

Table 5. Distribution of chemical elements in the ZrO2–20 wt.% SiC composite for point 1

Элемент	Весовой %	Атомный %
C K	2.28	7.95
O K	20.21	52.84
Si K	3.56	5.3
Zr L	73.95	33.91

Table 6. Distribution of chemical elements in the ZrO2–20 wt.% SiC composite for point 2

Элемент	Весовой %	Атомный %
C K	19.45	39.80
O K	7.18	11.04
Si K	48.52	42.47
Zr L	24.85	6.7

In Table 7 presents of the mechanical properties of sintered composites with SiC.

Table 7. Mechanical properties of sintered composites with SiC

Composite composition	Sintering temperature, °C	Relative density	Hardness HV_{10}, GPa	Fracture toughness K_{1C}, MPa·m$^{1/2}$
ZrO_2 – 10 wt.% SiC	1500	0.96	13.2±0.03	12.0±0.1
ZrO_2 – 20 wt.% SiC	1500	0.98	13.4±0.03	12.5±0.1
ZrO_2 – 30 wt.% SiC	1500	0.98	13.5±0.03	12.8±0.1
ZrO_2 – 10 wt.% SiC	1600	0.98	13.5±0.03	13.1±0.1
ZrO_2 – 20 wt.% SiC	1600	0.99	13.6±0.03	13.3±0.1
ZrO_2 – 30 wt.% SiC	1600	0.99	13.6±0.03	13.3±0.1

From Table 7 it can be seen that silicon carbide has a strengthening effect on the mechanical properties of yttria stabilized zirconia and provides a more acceptable combination of hardness and crack resistance compared to Al2O3 and WC additives.

5. Conclusions

Various nanoadditives to zirconium dioxide affect, first of all, the hardness and strength of the composite as a whole. They increase these values in different ways, depending on their content and sintering conditions. Hot pressing by electrosintering, significantly activates the compaction process, contributes to the formation of a finely dispersed microstructure. The mechanism of the sintering process occurs in different ways, depending on the ability to conduct electric current, hardening additives.

Based on a study on the sintering of composites based on zirconium oxide with additives of aluminum oxide, tungsten monocarbide and silicon carbide, it can be concluded that from the point of view of increasing strength, in particular fracture toughness, aluminum oxide additives are more effective; from the point of view of increasing hardness and at the same time fracture toughness, composites with additives of silicon carbide are more promising.

Thus, it is possible to propose the creation of a functional gradient material, the top layer of

which will be from ZrO2–Al2O3, the middle layer ZrO2–SiC, and the lower layer ZrO2–WC. The material can have a multifunctional application, one of the most promising applications would be the production of laminated inserts for cutting tools. The question of selecting the optimal composition for each layer will be determined by the operating conditions of this material.

Funding: The researches were co-financed by Ministry of Education and Science of Ukraine project No. 0121U109441.

References

1. A.I. Gusev, A.S. Kurlov, Production of nanocrystalline powders by high-energy ball milling: model and experiment. Nanotechnology 19, 26 (2008) 265–302.

2. S.N. Kulkov, S.P. Buyakova, I.S. Konovalenko, Osobennosti fragmentatsii chastits ZrO2 pri mehanicheskoy obrabotke. Pisma v ZhTF 35, 3 (2009) 67–73 (in Russian).

3. X. Chena, L. Liub, Y. Donga, Preparation of nano-sized Bi2Te3 thermoelectric material powders by cryogenic grinding. Progress in Natural Science. Materials International 22, 3 (2012) 201–206.

4. B.K. Vanleeuwen, K.A. Darling, C.C. Koch, R.O. Scattergood, Novel technique for the synthesis of ultra-fine porosity metal foam via the inclusion of condensed argon through cryogenic mechanical alloying. Materials science and Engineering: A. Structural Materials 528, 4–5 (2011) 2192–2195.

5. J. Yang, Y. Wang, R.N. Dave, R. Pfeffer, Mixing of nano-particles by rapid expansion of high-pressure suspensions. Advanced Powder Technology 14, 4 (2003) 471–493.

6. E. Gevorkyan, V. Nerubatskyi, V. Chyshkala, O. Morozova, Revealing specific features of structure formation in composites based on nanopowders of synthesized zirconium dioxide. Eastern-European Journal of Enterprise Technologies 5, 12(113) (2021) 6–19. DOI: 10.15587/1729-4061.2021.242503.

7. V.O. Chyshkala, S.V. Lytovchenko, V. P. Nerubatskyi, R. V. Vovk, E.S. Gevorkyan, O.M. Morozova, Detection of regularities of Y2Zr2O7 pyrochlor phase formation during the reaction of solid-phase synthesis under different temperature-time conditions. Functional Materials 29, 1 (2022) 30–38. DOI: 10.15407/fm29.01.30.

8. A. Suresh, M.J. Mayo, Crystallite and Grain-Size-Dependent Phase Transformations in Yttria-Dopped Zirconia. Journal of the American Ceramic Society 86, 2 (2003) 360–362.

9. D.-J. Chen, M.J. Mayo, Densification and grain growth of ultrafine 3 mol.% Y2O3–ZrO2 ceramics. Nanostructure Materials 2 (1993) 469–478.

10. Y. Sakka, T. Suzuki, K. Morita, Colloidal processing and superplastic properties of zirconia and alumina-based nanocomposites. Scripta Materials 44 (2001) 2075–2078.

11. E.S. Gevorkyan, V.P. Nerubatskyi, R.V. Vovk, V.O. Chyshkala, S.V. Lytovchenko, O.M. Morozova, J.N. Latosinska, Features of synthesis of Y2Ti2O7 ceramics for the purpose of obtaining dispersion-strengthened steels. Acta Physica Polonica A 142, 4 (2022) 529–538. DOI: 10.12693/APhysPolA.142.529.

12. A.A. Ilicheva, S.V. Kutsev, L.I. Podzorova, Morfologicheskie osobennosti nanoporoshkov sistemyi ZrO2 – Al2O3 – CeO2 v zavisimosti ot usloviy polucheniya prekursorov. Steklo i keramika 10 (2009) 26–29 (in Russian).

13. M.D. Matthews, K.A. Pechenik, Rapid hot pressing of ultrafine PSZ powders. Journal of

American Ceramics Society 74, 4 (1991) 1547–1553.

14. E.S. Gevorkyan, M. Rucki, A.A. Kagramanyan, V.P. Nerubatskiy, Composite material for instrumental applications based on micro powder Al2O3 with additives nano-powder SiC. International Journal of Refractory Metals and Hard Materials 82 (2019) 336–339. DOI: 10.1016/j.ijrmhm.2019.05.010.

15. E. Gevorkyan, V. Nerubatskyi, Yu. Gutsalenko, O. Melnik, L. Voloshyna, Examination of patterns in obtaining porous structures from submicron aluminum oxide powder and its mixtures. Eastern-European Journal of Enterprise Technologies 6, 6(108) (2020) 41–49. DOI: 10.15587/1729-4061.2020.216733.

16. J. Sun, C. Huang, J. Wang, H. Liu, Mechanical properties and microstructure of ZrO2 – TiN – Al2O3 composite ceramics. Materials Science and Engineering: A 416, 1–2 (2006) 104–108.

17. G.V. Samsonov, I.M. Vinnitskiy, Tugoplavkie soedineniya. Metallurgiya (1976) 556 (in Russian).

18. E. Gevorkyan, A. Mamalis, R. Vovk, Z. Semiatkowski, D. Morozow, V. Nerubatskyi, O. Morozova, Special features of manufacturing cutting inserts from nanocomposite material Al2O3-SiC. Journal of Instrumentation 16, 10 (2021) P10015. DOI: 10.1088/1748-0221/16/10/P10015.

19. E.S. Gevorkyan, V.P. Nerubatskyi, R.V. Vovk, O.M. Morozova, V.O. Chyshkala, Yu.G. Gutsalenko, Revealing thermomechanical properties of Al2O3–C–SiC composites at sintering. Functional Materials 29, 2 (2022) 193–201. DOI: 10.15407/fm29.02.193.

20. P. Palmero, Structural Ceramic Nanocomposites: A Review of Propertiesand Powders' Synthesis Methods. Nanomaterials 5, 2 (2015) 656–696. DOI: 10.3390/nano5020656.

21. M. Yoshimura, T. Ohji, M. Sando, Synthesis of nanograined ZrO2-based composites by chemical processing and pulse electric current sintering. Materials Letters 38, 1 (1999) 18–21.

22. M. Tokita, Mechanism of Spark Plasma Sintering. Journal of Materials Science 5, 45 (2004) 78–82.

23. M. Yoshimura, T. Ohji, M. Sando, Synthesis of nanograined ZrO2-based composites by chemical processing and pulse electric current sintering. Materials Letters 38, 1 (1999) 18–21.

24. T.S. Srivatsan, B.G. Ravi, A.S. Naruka, The microstructure and hardness of molybdenum powders consolidated by plasma pressure compaction. Journal of powder technology 114 (2001) 136–144.

25. S.V. Lytovchenko, E.S. Gevorkyan, V.P. Nerubatskyi, V.O. Chyshkala, L.V. Voloshyna, A study of the peculiarities of molding and structure formation of compacted multicomponent silicide composites. Journal of Superhard Materials 44, 3 (2022) 176–190. DOI: 10.3103/S1063457622030054.

26. H.C. Kim, I.J. Shon, J.E. Garay, Z.A. Munir, Consolidation and properties of binderless submicron tungsten carbide by field-activated sintering. International Journal of Refractory Metals and Hard Materials 22, 6 (2004) 257–264.

27. U. Anselmi-Tamburini, J.E. Garay, Z.A. Munir, Fast low-temperature consolidation of nanometric ceramic materials. Scripta Materialia 54 (2006) 823–828.

28. D. Jiang, O. Van der Biest, J. Vleugels, ZrO2–WC nanocomposites with superior properties. Journal of the European Ceramic Society 27 (2007) 1247–1251.

29. B. Basu, T. Venkateswaran, D. Sarkar, Pressureless sintering and tribological properties of WC–ZrO2 composites. Journal of the European Ceramic Society 25 (2005) 1603–1610.

30. G. Ann'e, S. Put, K. Vanmeensel, D. Jiang, J. Vleugels, O. Van der Biest, Hard, tough and strong ZrO2–WC composites from nanosized powders. J. Eur. Ceram. Soc. 25 (2005) 55–63.

31. J.-Y. Kim, S. Okamoto, N. Uchida, K. Uematsu, Hot isistatic pressing of Y-TZP powder compacts. Journal of Materials Science 25 (1990) 4634–4638.

32. A.I. Raychenko, Osnovyi protsessa spekaniya poroshkov propuskaniem elektricheskogo toka. Metallurgiya (1987) 128 (in Russian).

33. Patent na korisnu model 72841 Ukraine, MPK (2012.01) B22F 3/00. PristrIy dlya garyachogo presuvannya poroshkIv shlyahom pryamogo propuskannya elektrichnogo strumu / M.O. Azarenkov, E.S. Gevorkyan ta in.; zayavnik i patentovlasnik Gevorkyan E.S. # u201203031; zayavl. 15.03.12; opubl. 27.08.12, Byul. # 16 (in Ukrainian).

34. Z. Krzysiak, E. Gevorkyan, V. Nerubatskyi, M. Rucki, V. Chyshkala, J. Caban, T. Mazur, Peculiarities of the phase formation during electroconsolidation of Al2O3–SiO2–ZrO2 powders mixtures. Materials 15, 17 (2022) 6073. DOI: 10.3390/ma15176073.

35. I. Radko, M. Marhon, Features of research of grip strength composite materials contact with electrical worn parts. Machinery and Energetics 252 (2016) 176–185.

36. E. Gevorkyan, V. Nerubatskyi, V. Chyshkala, Y. Gutsalenko, O. Morozova, Determining the influence of ultra-dispersed aluminum nitride impurities on the structure and physical-mechanical properties of tool ceramics. Eastern-European Journal of Enterprise Technologies 6, 12(114) (2021) 40–52. DOI: 10.15587/1729-4061.2021.245938.

37. G. D. Quinn, Fracture toughness of ceramics by the vickers indentation crack length method: a critical review. Mechanical Properties and Performance of Engineering Ceramics II: Ceramic Engineering and Science Proceedings 27 (2006). DOI: 10.1002/9780470291313.ch5.

38. E. Gevorkyan, L. Cepova, M. Rucki, V. Nerubatskyi, D. Morozow, W. Zurowski, V. Barsamyan, K. Kouril, Activated sintering of Cr2O3-based composites by hot pressing. Materials 15, 17 (2022) 5960. DOI: 10.3390/ma15175960.

39. O.V. Karban, E.N. Hazanov, O.L. Hasanov, Nasledstvennost i modifikatsiya nanostrukturnoy keramiki ZrO2 v protsesse izgotovleniya. Perspektivnyie materialyi 6 (2010) 76 (in Russian).

40. E.S. Gevorkyan, V.P. Nerubatskyi, R.V. Vovk, V.O. Chyshkala, M.V. Kislitsa, Structure formation in silicon carbide – alumina composites during electroconsolidation. Journal of Superhard Materials 44, 5 (2022) 339–349. DOI: 10.3103/S1063457622050033.

41. Y. Sakka, T. Suzuki, K. Morita, Colloidal processing and superplastic properties of zirconia and alumina-based nanocomposites. Scripta Materials 44 (2001) 2075–2078.

42. J. Yang, Y. Wang, R. Dave, R. Pfeffer, Mixing of nano-particles by rapid expansion of high-pressure suspensions. Advanced Powder Technology 14, 4 (2003) 471–493.

43. M.D. Matthews, K.A. Pechenik, Rapid hot pressing of ultrafine PSZ powders. Journal of American Ceramics Society 74, 4 (1991) 1547–1553.

44. J. Grabis, I. Steins, D. Rasmane, Preparation and characterization of ZrO2–Al2O3 particulate nanocomposites produced by plasma technique. Proceedings of the Estonian Academy of Sciences, Engineering 12, 4 (2006) 349–357.

45. S.P. Buyakova, Yu.A. Horischenko, S.N. Kulkov, Struktura, fazovyiy sostav i morfologicheskoe stroenie plazmohimicheskih poroshkov ZrO2 (MgO). Ogneuporyi i tehnicheskaya keramika 6 (2004) 25–30 (in Russian).

46. E. Gevorkyan, M. Rucki, T. Salacinski, Z. Siemiatkowski, V. Nerubatskyi, W. Kucharczyk, Ja. Chrzanowski, Yu. Gutsalenko, M. Nejman, Feasibility of cobalt-free nanostructured WC cutting inserts for machining of a TiC/Fe composite. Materials 14, 12 (2021) 3432. DOI: 10.3390/ma14123432.

47. E. Gevorkyan, M. Rucki, Z. Krzysiak, V. Chishkala, W. Zurowski, W. Kucharczyk, V. Barsamyan, V. Nerubatskyi, T. Mazur, D. Morozow, Z. Siemiatkowski, J. Caban, Analysis of

the electroconsolidation process of fine-dispersed structures out of hot pressed Al2O3–WC nanopowders. Materials 14, 21 (2021) 6503. DOI: 10.3390/ma14216503.

48. A.K. Soh, D.-N. Fang, Z.-X. Dong, Analysis ofToughening Mechanisms of ZrO2 / nano-SiC CeramicComposites. J. Composite Mater. 38, 3 (2004) 227−241.

49. B.-Y. Ma, J. Yu, Phase composition of SiC–ZrO2 composite materials synthesized from zircon doped with La2O3. J. Rare Earths 27, 5 (2009) 806−810.

50. K. Houjou, K. Ando, K. Takahashi, Crack-healing behaviour of ZrO2 / SiC composite ceramics. International Journal of Structural Integrity 1, 1 (2010) 73–84. DOI: 10.1108/17579861011023810.